Electronic Supplementary Information

Active Guests in MoS_2 / $MoSe_2$ Host Lattice: Efficient Hydrogen Evolution Using Few-Layer Alloys of $MoS_{2(1-x)}Se_{2x}$

Vankayala Kiran, Debdyuti Mukherjee, Ramesh Naidu Jenjeti and Srinivasan Sampath*

Department of Inorganic and Physical Chemistry, Indian Institute of Science, Bangalore-560012, India

E-mail: sampath@ipc.iisc.ernet.in

Contents **Page**

Synthesis of bulk $MoS_{2(1-x)}Se_{2x}$ crystals

Bulk $MoS_{2(1-x)}Se_{2x}$ crystals with varying amount of x (0, 0.25, 0.5, 0.6, 0.75 and 1) have been prepared by high temperature solid state synthesis technique. Required amounts of elemental molybdenum, sulphur and selenium powders were mixed in stoichiometric proportions and sealed in an evacuated quartz tube. The quartz tube was heated at 800 ºC for 3 days to ensure the compound formation. The quartz tube was cooled down and opened to obtain the crystals.

Exfoliation of bulk crystals into few layer nanosheets

Few layer of $MoS_{2(1-x)}Se_{2x}$ were prepared by exfoliation of bulk sulfoselenide crystals.[1] Briefly, 50 mg of the bulk crystals were dispersed in 10 mL of water-ethanol mixture (6:4 ratio by volume) and sonicated for 6 h. The moderately stable colloidal dispersions were centrifuged at 4000 rpm for 20 min. to remove bulky, unexfoliated material. Very stable, clear supernatant contained large quantities of $MoS_{2(1-x)}Se_{2x}$ flakes. The concentration of the dispersion was calculated by knowing the amount settled down after centrifugation.

Electrochemical studies

All electrochemical measurements were carried out in cleaned glassware. Electrochemical measurements were carried out using an electrochemical workstation (CH 660C, USA) in a standard three-electrode cell with glassy carbon (GC) coated with various samples as the working electrode (WE), saturated calomel electrode (SCE) as reference and large area Pt foil as counter electrodes. The WE was prepared by drop coating an aliquot of above dispersions onto GC disk electrode (3 mm diameter), yields a constant catalsyt loading of 180 μg/cm^2. and dried under ambient conditions. Comparative stuides were carried out using bulk crystals that are coated onto GC electrodes. A known amount of bulk $MoS_2(1\text{-}x)Se_{2x}$ crystals were dispersed in ethanol and an aliuquot of the dispersion was drop casted onto GC electrode to yield a constant loading of 180 μg/cm^2. Linear sweep voltammetry (LSV) was recorded at a scan rate of 1 mV s^{-1} at 25°C in 0.5 M H_2SO_4. Prior to the measurements, the electrolyte was de-aerated by continuously purging with high purity N_2 gas for 30 min. The stability of the catalysts were determined by cyclic voltammetry (CV) carried out at a scan rate of 100 mVs^{-1} for 1000 cycles. All the electrochemical measurements were iR-corrected until otherwise specified. All the potentials were referred to reversible hydrogen electrode (RHE) by calibrating the SCE for reversible hydrogen potential using Pt as working and counter electrodes in 0.5M H_2SO_4, purged with high pure hydrogen gas

during the measurement.[2] The potential of SCE is related to RHE by the following equation based on the following figure.

$$E(RHE) = E(SCE) + 272\ mV \quad (1)$$

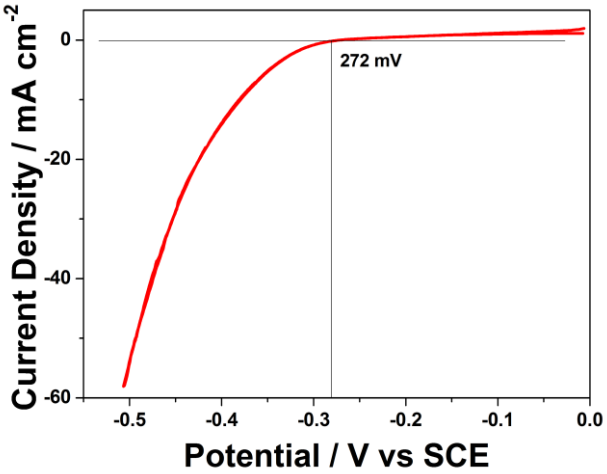

Figure Sa: calibration plot showing the potential of SCE with respect to RHE recorded in H_2-saturated 0.5 M H_2SO_4.

Characterization

Morphology of the materials were analyzed by scanning electron microscopy (SEM) (Carl Zeiss ultra 55) equipped with energy dispersive X-ray spectroscopy (EDS). Transmission electron microscopy (TEM) images were obtained using JEOL 2100F operating at 200 kV. The TEM samples were prepared by drop coating the diuluted dispersion on carbon-coated copper grid and dried under vacuum for 12 h. X-ray diffraction (XRD) patterns were recorded using Philips (PAN analytical) instrument (Cu-Kα radiation). Raman spectra were recorded using LabRAM (Horiba Jobin Yvon) instrument with an excitation wavelength of 514.5 nm and 50x long working distance objective. X-ray photoelectron spectroscopic analysis was performed on a Kratos Axis Ultra DLD X-ray photoelectron spectrometer with monochromatic Al kα (1486.708 eV) radition. Atomic force microscopy (TEM) images were obtained in Tapping mode using Veeco, Nanoscope IVa Multimode AFM using silicon nitride (Si3N4) probes with length of 130 μm, width of 35 μm, resonance frequency of 270 kHz and a force constant of 4.5 N/m.

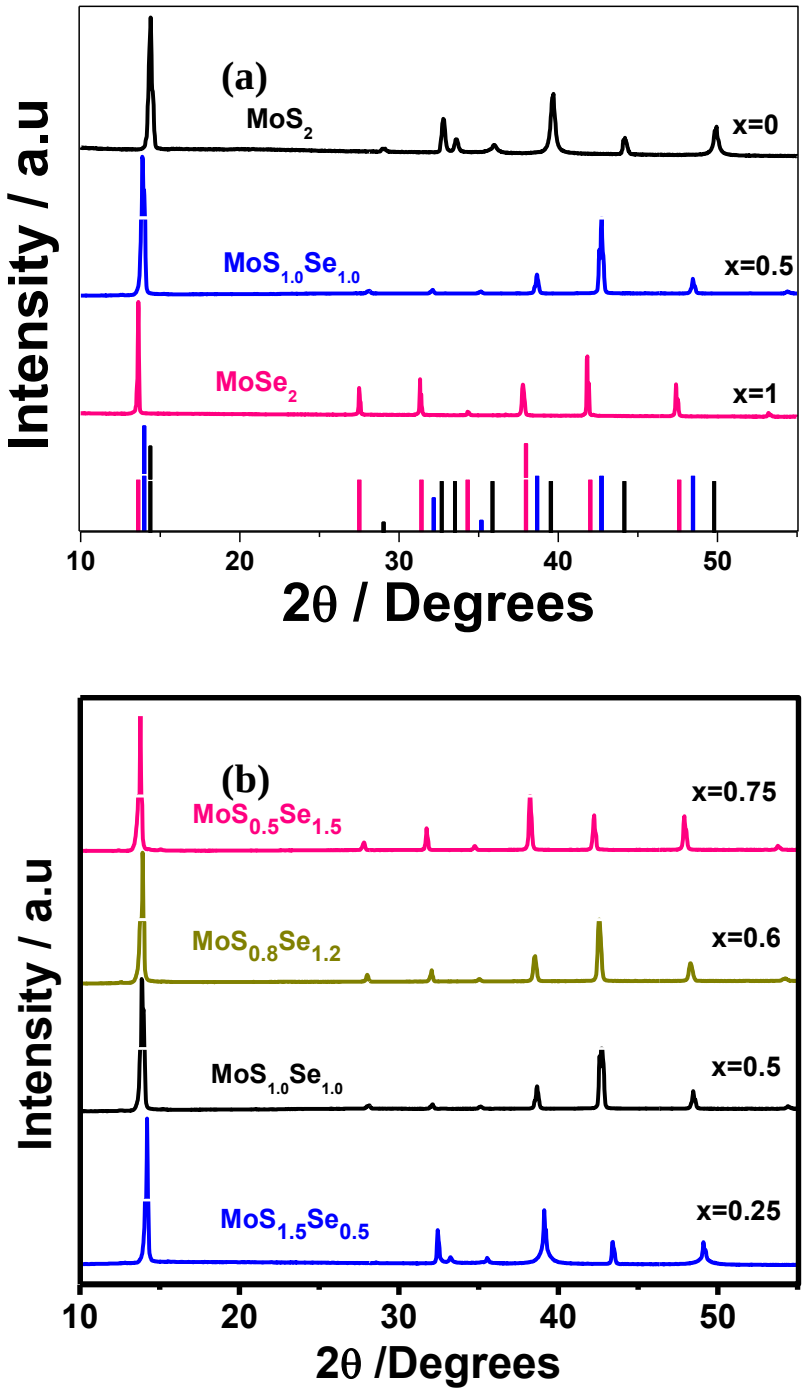

Figure S1. (a) X-ray diffraction patterns of MoS_2 (black), $MoS_{1.0}Se_{1.0}$ (blue) and $MoSe_2$ (pink). Corresponding JCPDF patterns for MoS_2 (37-1492), $MoSe_2$ (29-0914) and $MoS_{1.0}Se_{1.0}$ (36-1408) are given in the figure. (b) represents XRD patterns of Se incorporated MoS_2 of various compositions.

MoS_2 and $MoSe_2$ are known to crystallize in hexagonal structure with space group $P6_3/mmc$ (D_{6h}^4). The fundamental coordination for Mo is trigonal prismatic. Long range, weak van der Waal's forces between the layers hold the crystal in-tact. The $MoS_{2(1-x)}Se_{2x}$

alloys form simple structures similar to that of MoS_2 and $MoSe_2$.[1] A range of compositions has been prepared with S rich as well as Se rich phases. The XRD patterns of $MoS_{2(1-x)}Se_{2x}$ with varying x are given in figure S1(b). The reflections match well with the reported XRD patterns for x=0.25 (JCPDF No. 36-1409), x=0.5 (JCPDF No. 36-1408) and x=0.75 (JCPDF No. 36-1410). As shown in the figure, the (002) reflection shifts to lower 2Θ values with increase in Se content. A plot of lattice parameter with composition (figure S2) follows Vegard's law, an indication of the mixing of the components. The conservation of bond length in the alloys is due to small ratio of bond bending force to bond stretching force. Due to this reason, the M-S/Se bonds can also bend rather easily.

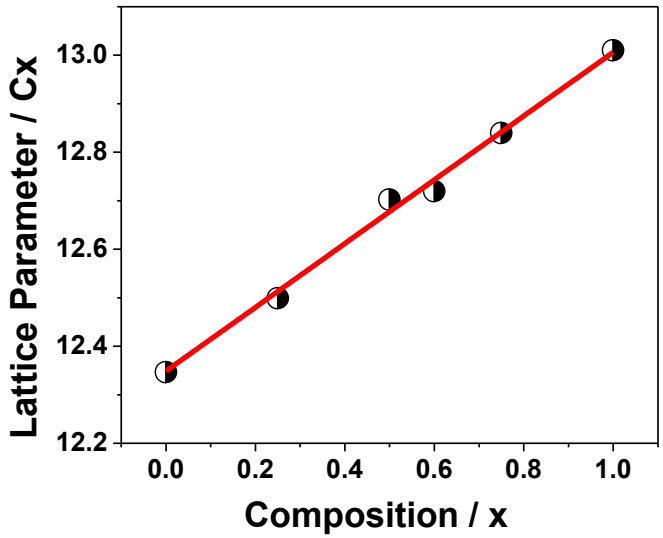

Figure S2. Variation of lattice parameter with composition. (002) reflection is used to calculate lattice parameter.

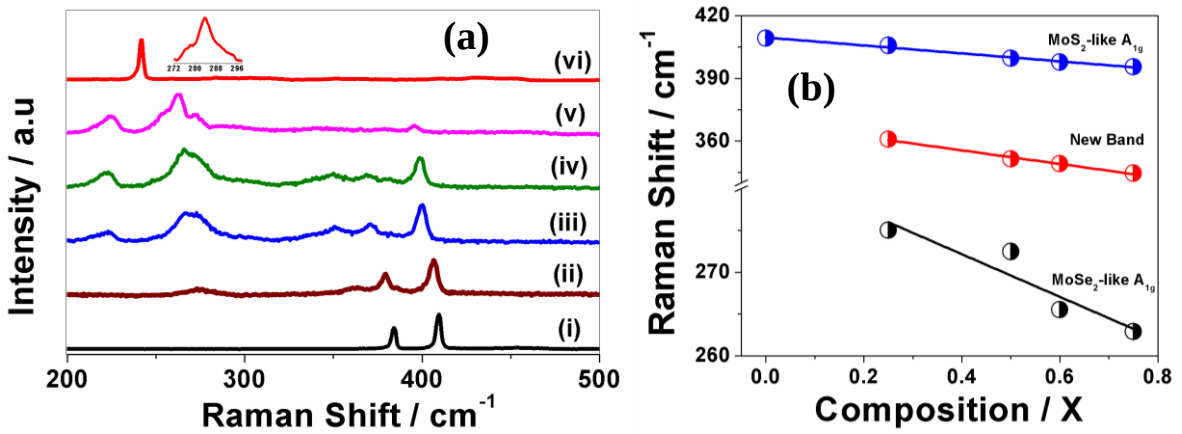

Figure S3. (a) Raman spectra of various compositions of $MoS_{2(1-x)}Se_{2x}$ with (i) x= 0, (ii) 0.25, (iii) x=0.5, (iv) x=0.6, (v) x=0.75 and (vi) x=1. The laser excitation wavelength used is 514 nm. Inset shows the expanded region of E_{2g} band of $MoSe_2$ located at 283.7 cm^{-1}. (b) Variation of band position with Se composition.

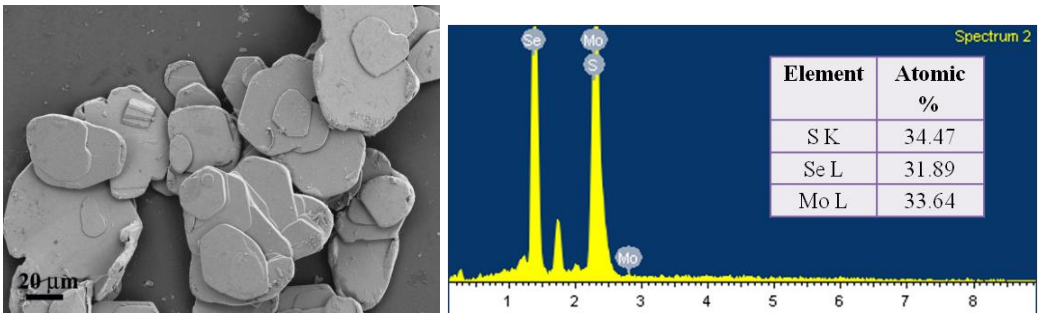

Figure S4. FE SEM image and corresponding EDS of bulk $MoS_{1.0}Se_{1.0.}$ The unlabelled peak at 1.7 keV originated from Si substrate.

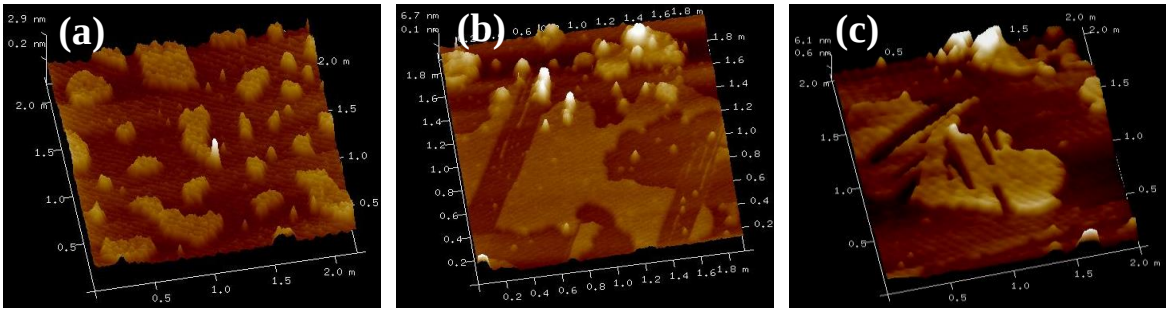

Figure S5. Tapping mode AFM images of few layer (a) $MoS_{1.0}Se_{1.0}$,(b) MoS_2 and $MoSe_2$ nanosheets.

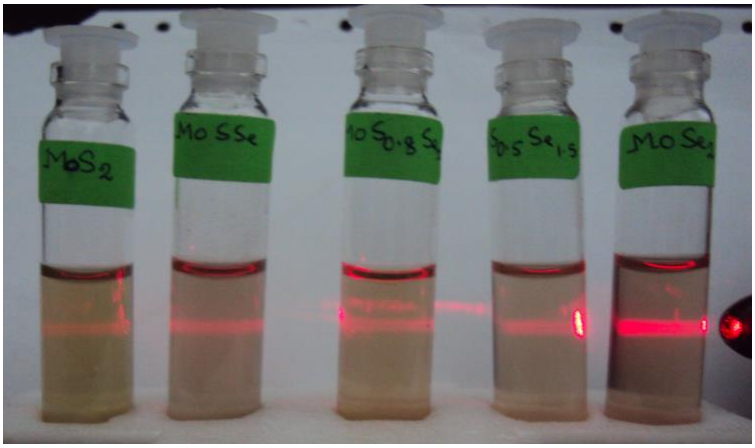

Figure S6. Digital photographs of $MoS_{2(1-x)}Se_{2x}$ dispersions depicting Tyndall light scattering effect.

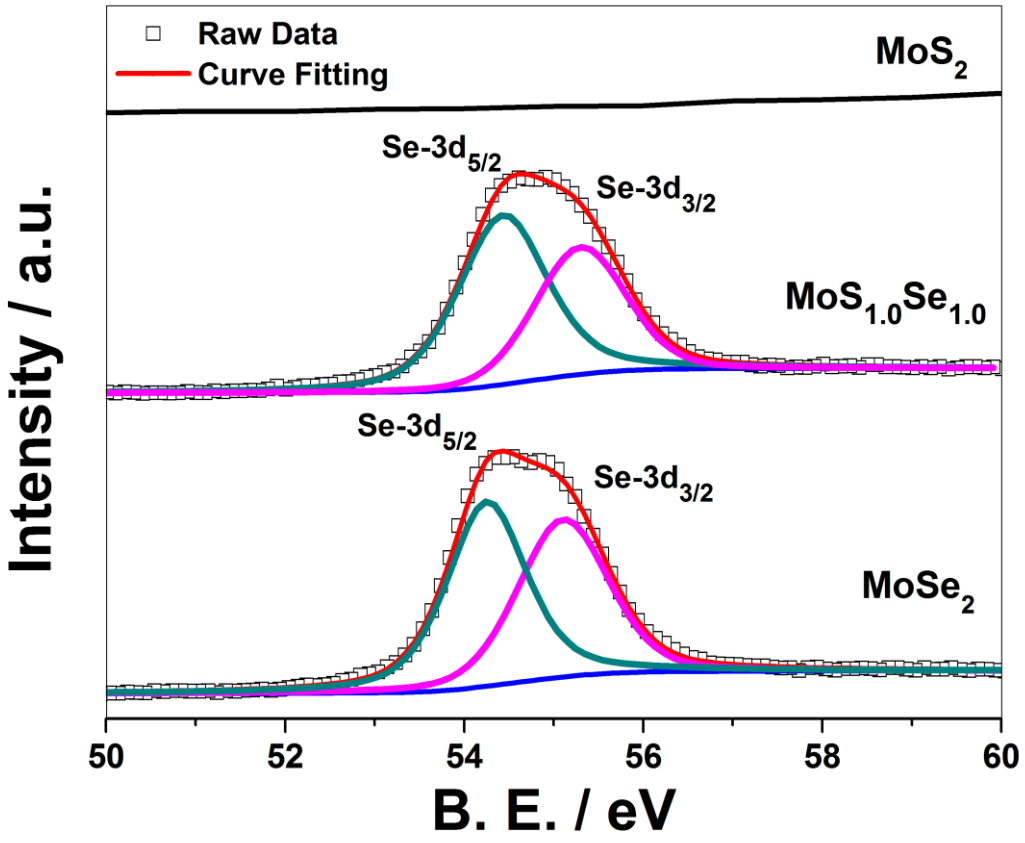

Figure S7. Deconvoluted XPS spectra of $MoS_{2(1-x)}Se_{2x}$ corresponding to Se-3d region for x=0 (top), x=0.5 (middle) and x=1 (bottom) of $MoS_{2(1-x)}Se_{2x}$.

Quantitative XPS analysis

The amount of sulfur and selenium present in $MoS_{2(1-x)}Se_{2x}$ composites is quantified using the following equation.

$S/Se = (I_S * F_{Se}) / (I_{Se} * F_S)$

where,

I_S and I_{Se} are the areas under the peaks for S-$2p_{3/2}$ and Se-$3p_{3/2}$ respectively.

F_S and F_{Se} are the relative symmetric factors (R.S.F) for S-$2p_{3/2}$ and Se-$3p_{3/2}$ respectively.[3]

R.S.F of S-2p3/2 = 0.4453

R.S.F of Se-3p3/2 = 0.84933

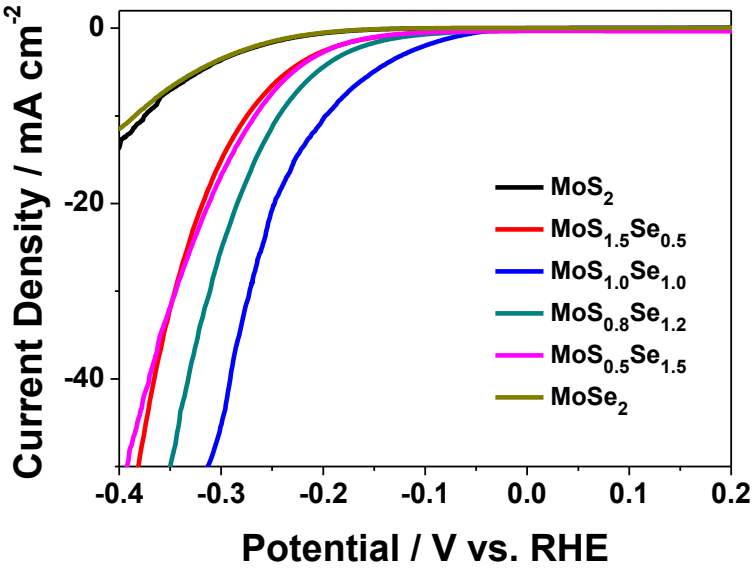

Figure S8. Linear sweep voltammograms of few layer $MoS_{2(1-x)}Se_{2x}$ with varying x. Electrolyte used is N_2-saturated 0.5 M H_2SO_4 and the scan rate used is 1 mV/sec.

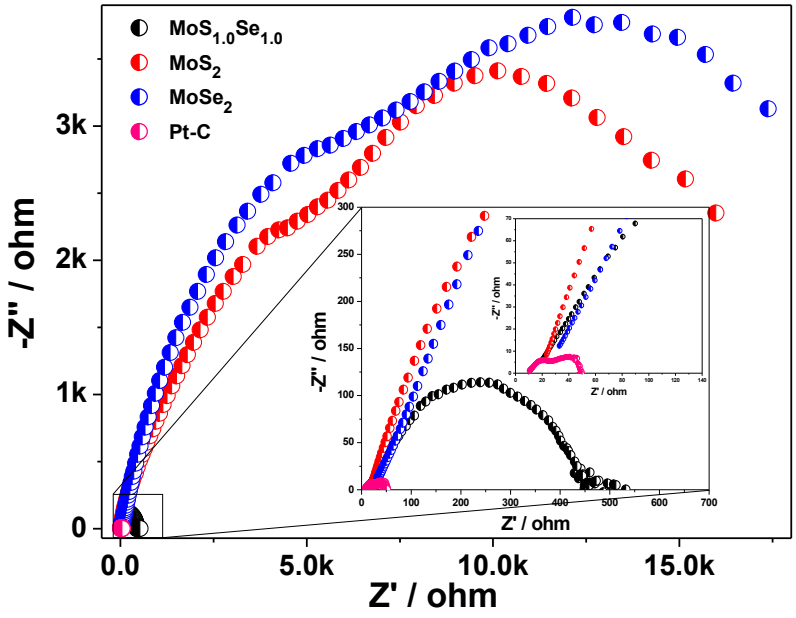

Figure S9. AC impedance data obtained -0.13 V vs. RHE in 0.5 M H_2SO_4.

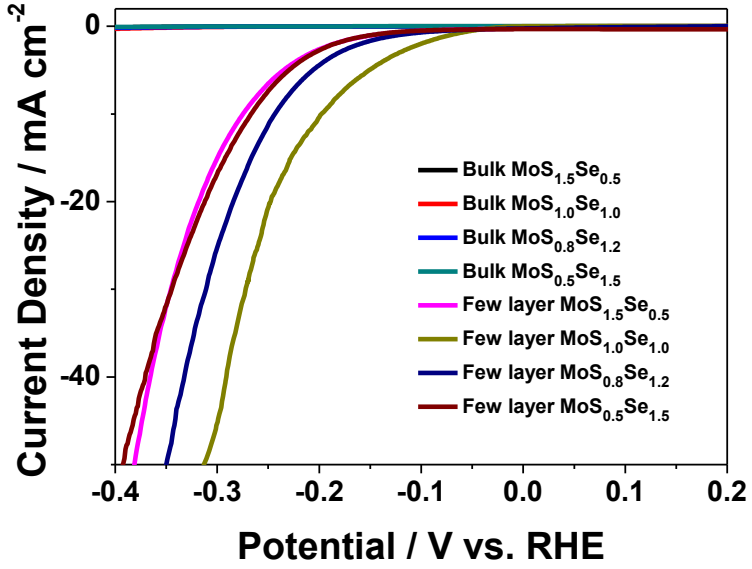

Figure S10. Linear sweep voltammograms of bulk and few layer $MoS_{2(1-x)}Se_{2x}$ with varying x. Electrolyte used is N_2-saturated 0.5 M H_2SO_4 and scan rate used is 1 mV/sec.

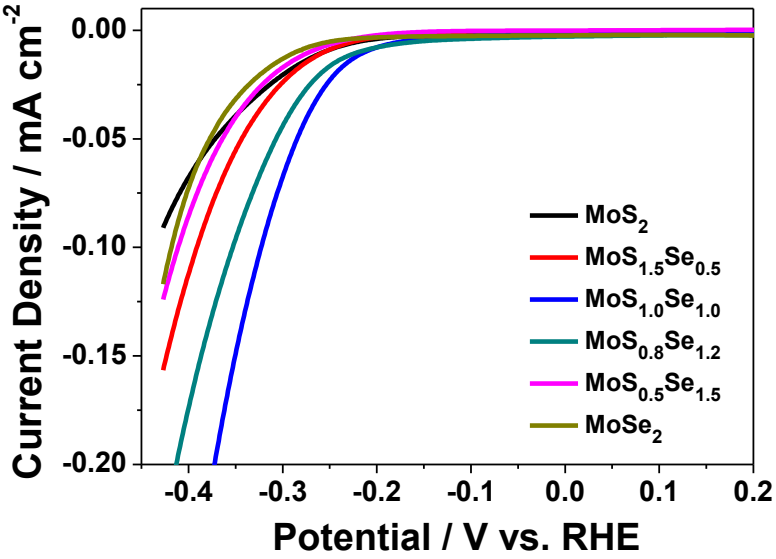

Figure S11. Linear sweep voltammograms of bulk $MoS_{2(1-x)}Se_{2x}$ with varying x. Electrolyte used is N_2-saturated 0.5 M H_2SO_4 and scan rate used is 1 mV/sec.

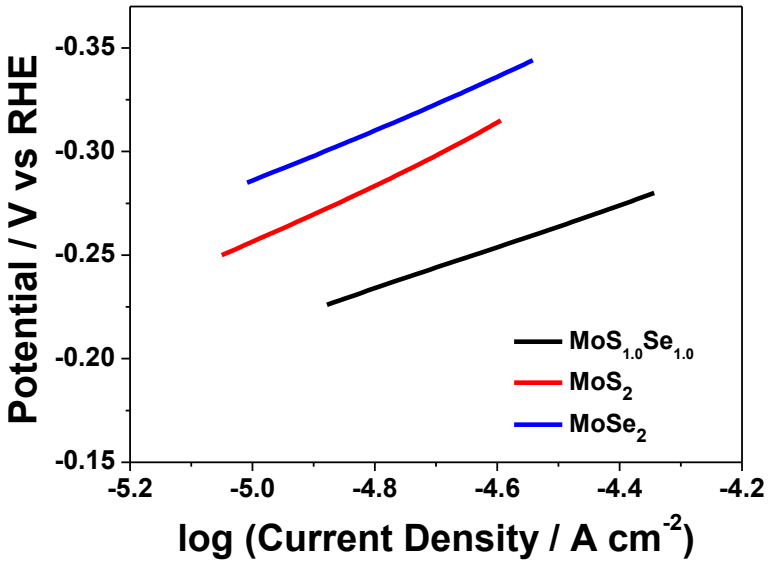

Figure S12. Tafel plots for HER on bulk $MoS_{2(1-x)}Se_{2x}$ crystals with x=0 (red), x=0.5 (black) and x=1 (blue).

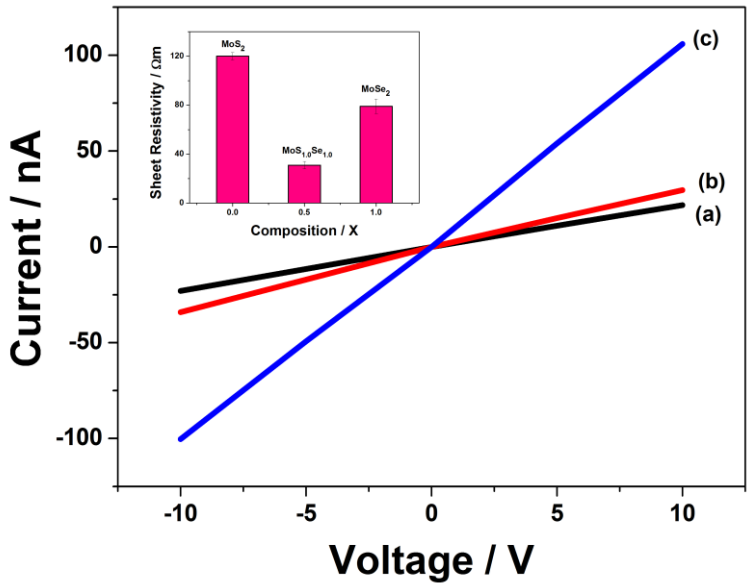

Figure S13. I-V data obtained at 25°C in 2-probe configuration for (a) MoS_2, (b) $MoSe_2$ and (c) $MoS_{1.0}Se_{1.0}$. Top inset shows sheet resistivity of $MoS_{2(1-x)}Se_{2x}$ measured in 4-probe van der pauw method. Bottom inset depicts schematic of the device used for measuring sheet resistivity.

Electrical properties of $MoS_{2(1-x)}Se_{2x}$ samples were measured in 2-probe and 4-probe configurations using Agilent Device Analyzer B1500A. To measure the electrical properties, samples were drop casted onto glass substrate which is coated with Al metal of thickness 150

nm by thermal evaporation technique at a pressure of $1x10^{-6}$ bar. A 0.5 μm gap is maintained between the electrodes. Figure S13 represents I-V data obtained at 25^{o}C for MoS_2, $MoSe_2$ and $MoS_{1.0}Se_{1.0}$ in 2-probe configuration. The data indicates that alloys possess high electronic conductivity as compared to pristine MoS_2 and $MoSe_2$.

In order to further strengthen the above argument, precise values of sheet resistances were measured using 4-probe methodology in van der pauw configuration (See inset). The sheet resistivity values are extracted by multiplying sheet resistance with the thickness of few layer $MoS_{2(1-x)}Se_{2x}$. The thickness of the material is measured from profilometer (sub-nanometric 3D non-contact optical profilometer, Taylor Hobson-surface profilers), which is around 335 nm. However, we found thicker regions (around 1-2 micron) in few places. A mean thickness is used for the calculation of sheet resistivity. As shown in the figure, the few layer $MoS_{1.0}Se_{1.0}$ possess lower sheet resistivity than that of MoS_2 and $MoSe_2$. In other words, few layer $MoS_{1.0}Se_{1.0}$ nanosheets are more conducting than pristine counterparts. The summary of electrical properties is given in table S4 (below).

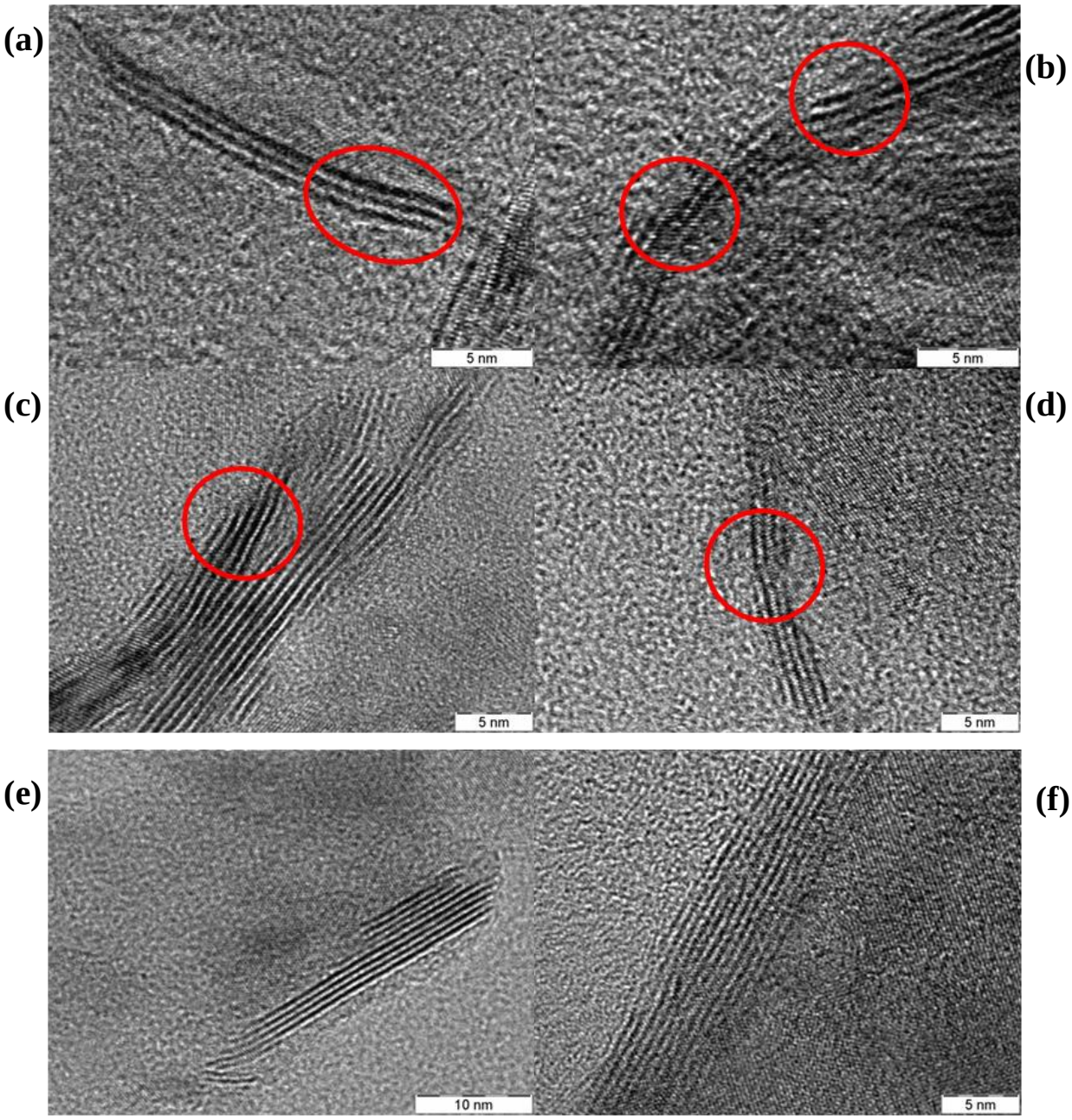

Figure S14. HRTEM images of fewlayer (a-d) $MoS_{1.0}Se_{1.0}$ and (e, f) MoS_2 nanosheets. Regions shown in red circles indicate some notable curvature in (002) layers.

Faradaic Efficiency Measurement

We have quantified the amount of hydrogen gas evolved as a function of time. Chronoamperometric experiment was carried out at -0.475 V vs. RHE using H-shaped electrochemical cell as shown in figure S13, to quantify the amount of gas evolved. The working electrode comprises of home-made glassy carbon electrode coated with catalyst material and the WE was kept in one compartment of H-shaped cell along with reference electrode (saturated calomel electrode). A large area counter electrode (Pt) was kept in the

other compartment. The quantity of gas evolved was measured using inverse burette method. It is observed that MoSSe can produce around 6 mL of hydrogen gas within 1 h. duration. The amount of gas evolved during the reaction is in close agreement with theoretical value, suggesting nearly 100% faradaic efficiency (figure S14). Theoretically, the amount of H_2 gas evolved can be calculated from the equation 1 based on Faraday's law

$$\text{Moles of } H_2 = \frac{1}{2}\,\frac{\int_0^t I\,dt}{F} \qquad (1)$$

where I is the applied current, t is the time and F is Faraday constant, 96485.34 C.

The hydrogen production efficiency of $MoS_{2(1-x)}Se_{2x}$ (for example, x=0.5) is found out to be superior to several reported catalysts such as MoS_3 particles, amorphous MoS_x prepared by electro-poymerization and MoS_2/reduced graphene oxide.[1,2]

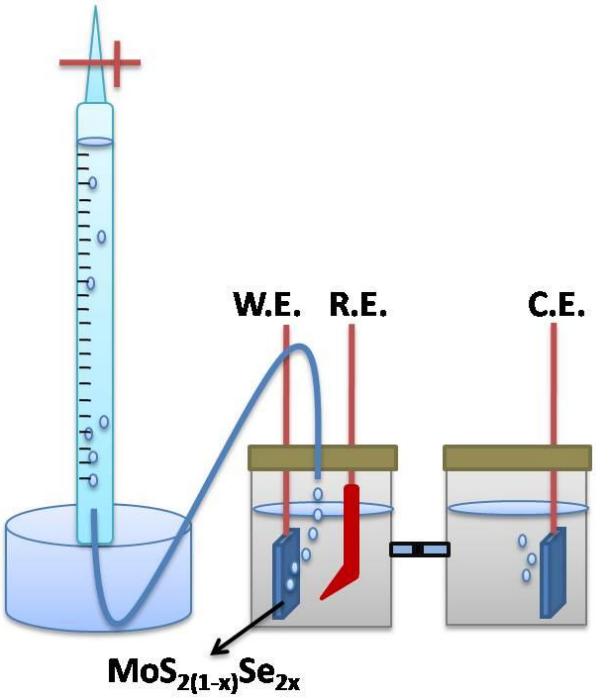

Figure S15. Schematic illustration of the setup used for measuring quantity of gas evolved.

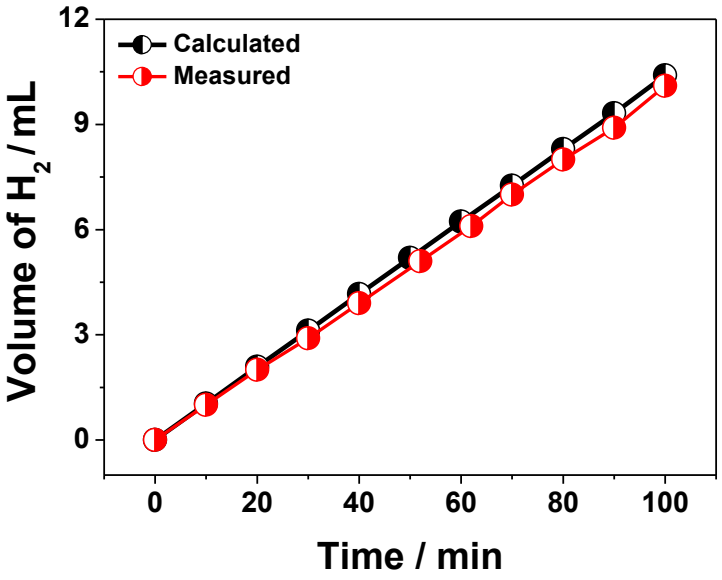

Figure S16. Quantity of H_2 gas evolved as a function of time for $MoS_{1.0}Se_{1.0}$ nanosheets. Black data points correspond to calculated numbers.

Table S1: Dynamic light scattering (DLS) data on $MoS_{2(1-x)}Se_{2x}$ with varying x. The hydrodynamic particle size distribution along with polydispersity is given.

Composition (x)	Hydrodynamic Size (nm)	Poly Disperse Index (PDI)
0	153	0.25
0.25	126	0.22
0.5	140	0.24
0.6	100	0.27
0.75	104	0.10
1	130	0.16

Table S2: Elemental ratio of S to Se for $MoS_{2(1-x)}Se_{2x}$ calculated from experimentally obtained XPS data.

Composition (X)	S : Se
0	1 : 0
0.25	1.49 : 0.5
0.5	0.98 : 1
0.6	0.8 : 1.2
0.75	0.52 : 1.5
1	0 : 1

Table S3: Electrochemical parameters obtained for $MoS_{2(1-x)}Se_{2x}$ with varying x.

Electrocatalyst	Tafel slope (mV/dec)	Exchange current density (A /cm^2)
MoS_2	96 ± 3	4.5×10^{-5}
$MoS_{1.5}Se_{0.5}$	87 ± 3	9.7×10^{-5}
$MoS_{1.0}Se_{1.0}$	56 ± 3	3.2×10^{-4}
$MoS_{0.8}Se_{1.2}$	86 ± 4	1.1×10^{-4}
$MoS_{0.5}Se_{1.5}$	88 ± 5	8.9×10^{-5}
$MoSe_2$	95 ± 4	3.6×10^{-5}
Pt/C	27 ±2	3.5×10^{-3}

Table S4. Summary of electrical properties of few layer $MoS_{2(1-x)}Se_{2x}$

	MoS_2	**$MoSe_2$**	**$MoS_{1.0}Se_{1.0}$**
Current at ±10 V (nA)	23 ± 2	34 ± 2	103 ± 4
Sheet Resistance (R in MΩ) (By Van der pauw method)	364 ± 10	240 ± 20	95 ± 10
Resistivity (ρ = R x d) (Ω m)	120 ± 3	79 ± 6	31 ± 3

References

1. K. –G. Zhou, N. –N. Mao, H. –X. Wang, Y. Peng, H. –L. Zhang, *Angew. Chem. Int. Ed.* 2011, **50,** 10839-10842.

2. M. –R. Gao, Z. –Y. Lin, T. –T. Zhuang, J. Jiang, Y. –F. Xu, Y. –R. Zheng, and S. –H. Yu, *J. Mater. Chem*., 2012**, 22**, 13662 - 13668.

3. http://www.xpsfitting.com/search/label/Relative%20Sensitivity%20Factors